The effect of soil and crop residue characteristics on polarimetric radar response

H. McNairn[a],*, C. Duguay[b], B. Brisco[c], T.J. Pultz[a]

[a]Canada Centre for Remote Sensing, 588 Booth Street, Ottawa, Ontario, Canada K1A 0Y7
[b]Département de Géographie, Université Laval, Cité Universitaire, Sainte-Foy, Québec, Canada G1K 7P4
[c]Noetix Research Inc., Suite 403, 265 Carling Avenue, Ottawa, Ontario, Canada K1S 2E1

Abstract

Although the interaction between linear polarized microwaves and agricultural targets has been studied extensively, far less is understood about the added information provided from polarimetric Synthetic Aperture Radars (SARs). Using 1994 Spaceborne Imaging Radar-C (SIR-C) data, this study examines the sensitivity of linear polarizations and polarimetric parameters to conditions present on agricultural fields during the period of preplanting and post harvest. The polarimetric parameters investigated include circular polarized backscatter, pedestal height, and co-polarized phase differences (PPD). The co-polarization signature plots are also discussed. Results indicate that the dominant scattering mechanism from these fields varies depending on the type and amount of residue cover, and whether the crop had been harvested. Radar parameters most sensitive to volume and multiple scattering perform best at characterizing these surface conditions. These parameters are the pedestal height, as well as the linear cross-polarization (HV) and the circular co-polarization (RR). The co polarization signature plots and the standard deviation associated with the PPD are also useful in categorizing these cover types. However, the field average PPD provides little information on residue and soil characteristics.

1. Introduction

For more than two decades, researchers have studied the response of microwaves to agricultural targets, including soil and crop parameters. These studies established that for nonvegetated surfaces, soil moisture, random and periodic surface roughness, and crop residue significantly affect radar backscatter. The vast majority of this research has been limited to the analysis of data acquired at one or more linear polarizations, from radars mounted on ground based platforms, aircraft, and satellites. Imagery from spaceborne Synthetic Aperture Radars (SARs) has been available over the last decade from a number of satellites including ERS-1, ERS-2, RADARSAT-1, and JERS-1. These spaceborne SARs transmit and receive microwaves in a single frequency and polarization.

In contrast, fully polarimetric radars record the complete characterization of the scattering field. Thus, not only are all four mutually coherent channels recorded (HH, VV, HV, and VH), but phase information is also retained during processing. Polarimetric SARs provide significantly more data relative to conventional radars that record backscatter only at the linear polarizations. Yet, the additional target information that could be provided by these fully polarimetric data sets is not well understood. The lack of understanding with regard to the application of these complex data is significant given the planned launch of satellites with fully polarimetric SAR sensors. These satellites include the Canadian RADARSAT-2, as well as the Japanese Advanced Land Observing System (ALOS), which will carry the PALSAR sensor (van der Sanden, Budkewitsch, Landry, Manore, McNairn, Pultz, & Vachon, 2000).

Many published studies on polarimetric applications have focused on target scattering mechanisms and have demonstrated the use of scattering parameters for general land cover classification (Evans, Farr, van Zyl, & Zebker, 1988; van Zyl, 1989). Although these studies have furthered our understanding of polarimetry, general land cover can be classified with far less complex data sets. As an example, crop type can be mapped using existing satellites that

acquire imagery at a single linear polarization, although multitemporal acquisitions are required (McNairn, Ellis, van der Sanden, Hirose, & Brown, in press). A significant improvement in crop type classification is achieved if the SAR data are acquired at multiple polarizations (McNairn, van der Sanden, Brown, & Ellis, 2000). However, the advantage of using complex polarimetric data for general land cover mapping has not been clearly established. In spite of this, polarimetric data could provide other advantages, specifically an improved sensitivity to soil and crop characteristics. Yet, the relationship between responses recorded by polarimetric sensors and these characteristics is not well understood.

2. Research objectives

In 1994, the Spaceborne Imaging Radar-C (SIR-C) SAR system was launched onboard the NASA Space Shuttle Endeavour (Stofan, Evans, Schmullius, Holt, Plaut, van Zyl, Wall, & Way, 1995). SIR-C acquired imagery simultaneously at C-Band (5.3 GHz) and L-Band (1.25 GHz). The sensor could operate in either dual polarization mode or quadrature (fully polarimetric) mode. During two 10-day flights in April and October of 1994, quadrature SIR-C data sets were acquired over a site located in western Canada, centred on Altona, Manitoba (49°4.9′N latitude, 97°39.6′W longitude).

These data were analyzed to determine the sensitivity of polarimetric parameters to agricultural targets. The SIR-C missions occurred during the period of preplanting and postharvest. Thus, soil characteristics (soil moisture and surface roughness) and residue characteristics (residue type and amount of residue) are the principal factors influencing radar response. The SAR information of primary interest in this research included backscatter at the linear and circular polarizations, the pedestal height, the co-polarization signature plots, and the co-polarized phase difference (PPD). The relationship between these radar parameters and the soil and residue characteristics is the focus of this article.

3. Review of selected polarimetric parameters

Upon interaction with a target, the incident electromagnetic wave can be depolarized and/or repolarized. Depolarization is the change in the degree of polarization of a fully or partially polarized wave, resulting in an increase (negative depolarization) or decrease (positive depolarization) in the unpolarized component of the wave. Unpolarized waves have equal amplitude orthogonal components and a random relative phase difference (Boerner, Mott, Lüneburg, Livingstone, Brisco, Brown, & Paterson, 1998). Depolarization is often a result of multiple scattering due to significant surface roughness, or volume scattering as occurs in dense vegetation. These targets exhibit a response that contains a large unpolarized component. If the polarization vector of the polarized component of the wave also changes, the wave is said to be repolarized (Boerner et al., 1998). In the specific case of linear cross-polarizations, the sensor records how much of the power from the transmitted linear wave (H or V) has been repolarized into the orthogonal polarization (V or H).

With fully polarimetric data nonlinear polarizations, such as the circular polarizations, can be synthesized. Circular polarizations are described in terms of their handedness relative to the observer. With right-handed circular waves (R), the electric field vector rotates clockwise. For left-handed waves (L), the vector rotates counterclockwise. With a single-bounce scatterer such as a smooth surface, the handedness of the received wave (relative to the observer) is opposite that of the transmitted wave. Thus, the circular cross-polarization (RL) is associated with these smooth surfaces (de Matthaeis, Ferrazzoli, Schiavon, & Solimini, 1992; Evans et al., 1988). In contrast, the circular co-polarization (RR or LL) responses are associated with volume or multiple scattering, and the handedness of the received wave (relative to the observer) is the same as that of the transmitted wave.

Pedestal height can also be derived from polarimetric data. The height of the pedestal is an indicator of the presence of an unpolarized scattering component, and thus the degree of polarization of a scattered wave. As indicated in Fig. 1, the pedestal can be visualized on the three-dimensional polarization signature plots generated from fully polarimetric data (van Zyl, Zebker, & Elachi, 1987). These plots characterize SAR responses at linear, circular, and elliptical polarized configurations. Because polarization signature plots capture many scattering characteristics of the target, at all polarizations, the shape of these plots is significant and can indicate the scattering mechanisms dominating the target response.

The polarization signature of a given pixel, as represented by the polarization plot, is the sum of the polarization

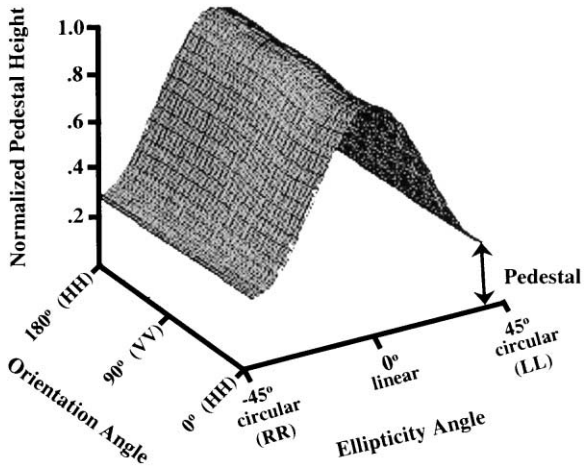

Fig. 1. Example of a co-polarization signature plot. These three-dimensional plots can be generated from fully polarimetric data and characterize SAR response at linear, circular, and elliptical polarized configurations. The pedestal height is also visualized on these plots.

signatures of many individual scatterers (Evans et al., 1988). If several scattering mechanisms are present in the target, then the individual polarization signatures are not identical and their nulls can occur at different polarizations. As a result, when the different polarization signatures for the individual scatterers are added, the nulls of the resultant signature are replaced by minima. This increases the minimum power at all polarizations. The co-polarization pedestal height is the ratio of the maximum to the minimum received intensity when the polarizations of the transmitting and receiving antenna are the same. Signatures with significant pedestals are typical of targets that are dominated by volume scattering or multiple surface scattering. Evans et al. (1988) reported that pedestal height was directly proportional to vegetation density. de Matthaeis et al. (1991), Ray, Farr, and van Zyl (1992), and van Zyl (1989) found that pedestal height was related to surface roughness with increases in roughness resulting in higher pedestals.

PPD originate from various sources including double-bounce scattering from within the target (Ulaby, Held, Dobson, McDonald, & Senior, 1987). A phase difference will also occur as a result of different electrical path lengths between the HH- and VV-polarized waves, when scatterers dominating VV-polarized backscatter are at a range different from those dominating HH-polarized backscatter. Phase differences can also result from a time delay when the phase velocity of H and V waves differs within the target. The PPD can be calculated from polarimetric data and some researchers have found a relationship between the phase difference and target characteristics. Hoekman, van der Sanden, and Vissers (1992) suggested that bare fields, stubble fields, and senesced cereals should have a mean phase difference close to zero, green crops of intermediate height a small phase difference, while for thick canopies like corn, phase differences would be appreciable. Indeed, Evans et al. (1988) reported that for relatively smooth surfaces dominated by single-bounce scattering, HH and VV are in phase and consequently, mean phase differences were close to zero. In contrast, double-bounce scatterers exhibited a phase shift between HH and VV of approximately 180°.

The standard deviation of the phase differences associated with the target, and not just the mean PPD, should be considered. Ulaby et al. (1987), as well as Kuga and Zhao (1996), found that the phases of HH and VV were highly correlated for surfaces with small roughness characteristics. For these smooth surfaces, the PPD fit a Gaussian distribution with a mean of zero. Sarabandi, Oh, and Ulaby (1991) suggested that the standard deviation of the phase difference would be a function of surface roughness. For targets where volume or multiple scattering dominates, phase differences vary from one scatterer to the next. In these cases, Kuga and Zhao (1996) observed phase differences uniformly distributed between $-180°$ and $+180°$. This distribution is due to multiple interactions within the target, which result in highly varying HH−VV phase differences (Evans et al., 1988).

4. Scattering mechanisms associated with distributed targets

According to Hoekman et al. (1992) the response recorded by a SAR sensor is often a result of a mixture of scattering mechanisms. This observation is confirmed by Baronti et al. (1995) who state that in general, several types of sources and scattering mechanisms are simultaneously present in backscatter from one target. For example, within a vegetation canopy stalks generate double-bounce scattering. Ensembles of inclined cylinders (i.e., stems) generate volume scattering with some multiple scattering. Leaves generate volume scattering.

Although several scattering mechanisms are often present within a distributed target, one mechanism—surface, double-bounce, or multiple/volume—usually dominates. When surface scattering dominates, VV-polarized backscatter is equal to or greater than HH backscatter, RL backscatter is significantly greater than RR and the PPD is approximately 0° (Baronti et al., 1995). The pedestal observed on the co-polarization plots is low, suggesting that very little depolarization of the incident wave occurs during surface scattering. Surface scattering is typical of bare fields that appear smooth relative to the wavelength.

A number of scattering sources are found within large biomass crop canopies like corn. Incident waves are scattered from the stalks, attenuated by the canopy and reflected from the ground. At L-Band, de Matthaeis, Schiavon, and Solimini (1994) suggest that cornstalks scatter downward both H and V polarizations, so that attenuation by the canopy and upward reflection from the ground result in higher HH backscatter relative to VV. Although double-bounce scattering within a corn canopy can dominate multiple, volume, and surface scattering often still contribute to the radar response. The SAR frequency and incidence angle will influence the mix of scattering mechanisms from these targets. For example, de Matthaeis et al. (1992) found only weak double-bounce at C-Band from a corn canopy since the presence of leaves attenuated the double-bounce contributions. van Zyl et al. (1987) indicated that at larger incidence angles, attenuation by the canopy is stronger and thus single and double scattering is reduced and volume scattering dominates. Targets that are dominated by double-bounce reflections have phase shifts approaching 180°.

Although surface scattering dominates smooth bare fields, fields that appear rough relative to the incident wavelength produce multiple scattering. Volume scattering occurs within dense vegetation canopies. When multiple or volume scattering dominates, the linear and circular co- and cross-polarized backscatter is approximately equal ($HH \approx VV$ and $RL \approx RR$) (Baronti et al., 1995). Volume

scattering from leaves can produce a RL/RR ratio slightly greater than 1. However, the parameters most indicative of multiple and volume scattering are the pedestal height and the variance associated with the PPD. Multiple and volume scattering result in HH and VV phase differences that vary over the target causing a random response. Pedestal height increases and the PPD distribution broadens. This indicates depolarization and an increase in the unpolarized component of the scattered wave.

5. Methodology

The land use and economy of southern Manitoba is based on intensive and diversified agricultural production. Agricultural crops grown across the Altona site include small cereal grains, sunflower, canola, flax, corn, sugar beets, potatoes, and specialty crops such as canary seed, peas, beans, and lentils. The topography of the region is generally level to very gently sloping. The dominant soil types of the study area are sandy loams to the west, changing to heavier clayey soils in the east.

Two SIR-C quadrature acquisitions (April 12 and October 5, 1994) were used in this analysis. In April, the Altona study site consisted of bare agricultural fields with varying surface roughness and amounts of crop residue cover. The site conditions in October were similar, although some crops had not yet been harvested. Thus, several fields of standing senesced corn and sunflowers were present during the second campaign.

Incidence angles were relatively large for both of these acquisitions. The incidence angle was approximately 44° at the centre of the site for the April image, and 51° for the October image. Slant range resolution for both acquisitions was approximately 5×13 m (azimuth $\times$ range). The SIR-C data were radiometrically calibrated by the Jet Propulsion Laboratory (JPL) as described in Freeman et al. (1995). Cross-swath calibration uncertainties for both missions were within 1 dB.

During both the April and October field campaigns, information on surface conditions was collected coincident with SAR acquisitions. Quantitative soil moisture, surface roughness, and residue measurements were made on 12 fields during the October SIR-C overpass (Pultz, Crevier, Brown, & Boisvert, 1997). Soil moisture measurements were taken ± 2 h of the SAR acquisition. Volumetric soil moisture (0–5 cm) was measured at five sample sites in each field. To represent conditions across the fields, these five sites were located at least 50 m apart, along a transect through the field. At each site, average soil moisture was calculated from three replicate measurements taken within 1 m of the centre of the site. Soil moisture was measured using a Time Domain Reflectometer (TDR). The TDR measures the soil dielectric values and these data are then converted to volumetric soil moisture using the method described in Topp, Davis, and Annan (1980).

Surface roughness was measured using the SRM-200 surface roughness meter. This instrument measures RMS height along a 50-cm length using a photographic technique (Johnson, Brisco, & Brown, 1993). Roughness was measured at a minimum of five sites per field, along a transect through the field. At each measurement site, average roughness was calculated from three replicate surface roughness measurements taken within 2–3 m of the centre of the site. Roughness measurements were made parallel to the SIR-C look direction.

The percent coverage of crop residue was estimated at each surface roughness measurement site using a line transect method. At least five sites were located in each field. Again, three replicate measurements were taken at each site as an estimate of average residue cover at that site. This particular line transect method used a 7-m knotted rope with 50 equally spaced knots (Coleman & Roberts, 1987). Each knot that lies directly above a piece of residue counts for 2% residue cover. This measurement strategy will accurately characterize residue levels across a field (Richards, Walter, & Muck, 1984).

Topographic variations across these fields were minimal and thus only small variations in roughness and residue cover were present within each field. Data from these 12 quantitative fields were used to establish the statistical relationship between surface conditions (soil moisture, surface roughness, and percent residue) and radar response (Table 1).

For both the April and October acquisitions, qualitative information was gathered on another 80–90 fields across the study site (Table 2). This information included residue type and a visual estimate of residue amount. Major residue categories included wheat, barley, lentils, sunflower, corn, canola, and peas. Residue type was verified using crop surveys completed during the 1993 and 1994 growing seasons. During the fall campaign, most fields of corn and sunflower had not yet been harvested and the location of these standing senesced fields was recorded. These observations captured a wide range of field conditions related to

Table 1
Field average data acquired on October 5, 1994

Field number	RMS (mm)	Percent residue	Volumetric soil moisture (0–5 cm)
1–1	14.15	26.4	15.8
1–2	19.65	51.2	16.3
1–3	13.20	33.4	28.3
2–1	15.50	67.6	15.7
2–2	13.00	19.6	16.2
2–3	10.15	37.4	17.4
3–1	20.60	22.4	13.6
3–2	9.10	42.6	14.7
3–3	11.90	3.6	14.7
4–1	22.35	10.4	19.1
4–2	16.45	23.6	25.0
4–3	12.25	34.4	23.2

Table 2
Number of qualitative fields listed according to percent residue cover

Residue categories	Number of fields	
	April	October
0–20%	15	36
21–40%	11	14
41–60%	30	12
61–80%	18	4
81–100%	16	4
Unharvested senesced corn	0	6
Unharvested senesced sunflower	0	5
Total number of fields	90	81

tillage and residue. No-till fields of lentil and pea residue had very smooth soil surfaces, but sparse and fine residue coverage. No-till fields of corn and sunflower had significantly more residue coverage, with larger pieces of residue. No-till wheat and barley residue is similar in size to bean residue, but these small grain crops generally leave much more residue cover. Many fields had also been tilled which increased surface roughness but reduced residue amounts. These varied field conditions were used to explore the information contained in both the co-polarization signature plots and the PPD.

Previous research has concluded that both crop and tillage row directions can significantly affect radar backscatter (McNairn et al., 1996). However, look direction effects are strongest near perpendicular and as the radar look direction decreases, these effects are also reduced (Brisco et al., 1991). Residue and tillage row directions across the study site generally followed the north–south and east–west field orientations predominant in southern Manitoba. Tillage and residue row direction was recorded on all fields surveyed, as well as on the 12 fields were measurements were acquired. A standard multiple range test established that for this particular data set, backscatter did not vary significantly (at a 95% probability level) among the study fields, as a function of row direction. Due to the orbital inclination of SIR-C (57°), the look direction effects for these SAR acquisitions were minimal.

The single look complex data were delivered by JPL in Compressed Stokes matrix format. The data were decompressed and then multilooked. The April and October scenes were processed to two and three looks, respectively, in order to reduce data volumes and to create relatively square pixels. Regions of interest (ROIs) were drawn over the quantitative and qualitative fields. Field average statistics, as well as co-polarization signature plots, were generated for these ROIs.

Polarization signature plots capture SAR responses at the linear, circular, and elliptical polarized configurations. Co-polarization signature plots represent the case where the transmitted and received polarizations are identical. Although many targets can produce similar plots, the shape of the plots as well as the pedestal on which the plots sit, provide clues about the type of scattering dominant from the target. The plot displays synthesized power as a function of the orientation (φ) and ellipticity (χ) angles of the waves transmitted to and scattered back from the target (Fig. 1). Circular polarizations have ellipticity angles of 45° with the sign of the ellipticity angle indicating the handedness or direction of rotation of the wave. Negative values indicate right-hand polarizations (R) and positive values indicate left-handed (L) polarizations. Linear polarizations have an ellipticity angle of 0°. Although all orientations are represented in the plot, the commonly used linear polarizations have orientation angles of 0° (H) or 90° (V).

6. Results and discussion

6.1. Regression analysis: the contribution of soil and residue characteristics to radar response

Both the simple linear and multiple linear regression results are presented in Table 3. As listed in Table 3, total power is the sum of the power recorded for each of the linear polarizations (HH, VV, HV, and VH). Given the relatively large incidence angle of the October 5th acquisition (51°), and the influence of both surface roughness and residue cover, surface soil moisture had no significant correlation with any of the radar parameters. At incidence angles larger than 30–40°, surface roughness (McNairn et al., 1996) and residue cover (McNairn et al., in press) significantly contribute to linear polarized radar backscatter.

Table 3
Simple and multiple regression results (October 5, 1994)

	Simple linear regression (R^2)			
	Volumetric soil moisture (0–5 cm)	Percent residue	Surface roughness (RMS)	Multiple linear regression[a] (R^2)
C-Band				
HH	.072	.295	.590*	.743*
VV	.046	.313	.568*	.709*
HV	.009	.438*	.419*	.643*
Total power	.052	.325	.579*	.732*
Pedestal height	.199	.478*	.419*	.872*
RL	.051	.298	.612*	.740*
RR	.006	.421*	.414*	.621
PPD	.022	.009	.425*	.458
L-Band				
HH	.036	.251	.593*	.824*
VV	.043	.204	.558*	.630
HV	.058	.413*	.629*	.840*
Total power	.041	.245	.592*	.679*
Pedestal height	.240	.362	.601*	.918*
RL	.040	.206	.563*	.632*
RR	.055	.368*	.630*	.805*
PPD	.059	.257	.459*	.601

[a] Independent variables include volumetric soil moisture, percent residue, and surface roughness.

* Statistically significant at a probability level less than .05.

Conversely, the influence of soil moisture on radar backscatter is reduced at these larger angles.

Percent residue cover was significantly correlated with several radar parameters sensitive to multiple or volume scattering. These parameters include cross-polarized linear backscatter, co-polarized circular backscatter, and pedestal height. None of the remaining radar parameters were significantly correlated with residue cover. These results suggest that multiple scattering is occurring on these fields. Residue clearly contributes to this scattering. However, although the simple regression model was significant for these radar parameters, the contribution of residue to radar response was only about 40%. Thus, a significant proportion of variance in the radar response remains unaccounted for.

In contrast, surface roughness was significantly correlated with the response recorded for each radar parameter. At L-Band, regression results among the radar parameters were very similar, although the R^2 value for the PPD was the weakest. In general, about 60% of the variance in L-Band radar response was explained by the variations in surface roughness. For C-Band, results were generally weaker with RL and HH backscatter most sensitive to surface roughness. L-Band results were stronger since these longer waves are able to penetrate the residue cover and interact directly with the underlying surface roughness.

When all three target variables were regressed against radar response using a multiple linear model, pedestal height provided the best results for both C- and L-Bands. Coefficients of determination for this variable were approximately 0.9. These results confirm that pedestal height is sensitive to multiple scattering on postharvest agricultural fields. The circular polarizations (RL at C-Band and RR at L-Band) also produced significant correlations. However, comparable results were obtained with HH, and thus in this context, the advantage of using circular polarizations rather than linear polarizations is not obvious.

6.2. Interpretation of the PPD

Both the simple and multiple regression results indicated that field average like-polarized phase differences (PPD) do not correlate well with conditions present on postharvest fields. This observation confirms results presented in Ulaby et al. (1987). Nevertheless, Boerner, Foo, and Eom (1987) hypothesized that the PPD could distinguish electrically flat from rugged and volumetric scattering targets. To further explore phase information, field average PPD were summarized in a frequency distribution plot (Fig. 2). Ulaby et al. (1987) reported that the distribution of the phase difference across a target might contain more information than that present in the mean phase statistic. Thus, field-based phase distribution plots were also generated, and plots for selective fields representative of the various classes are found in Figs. 3 and 4.

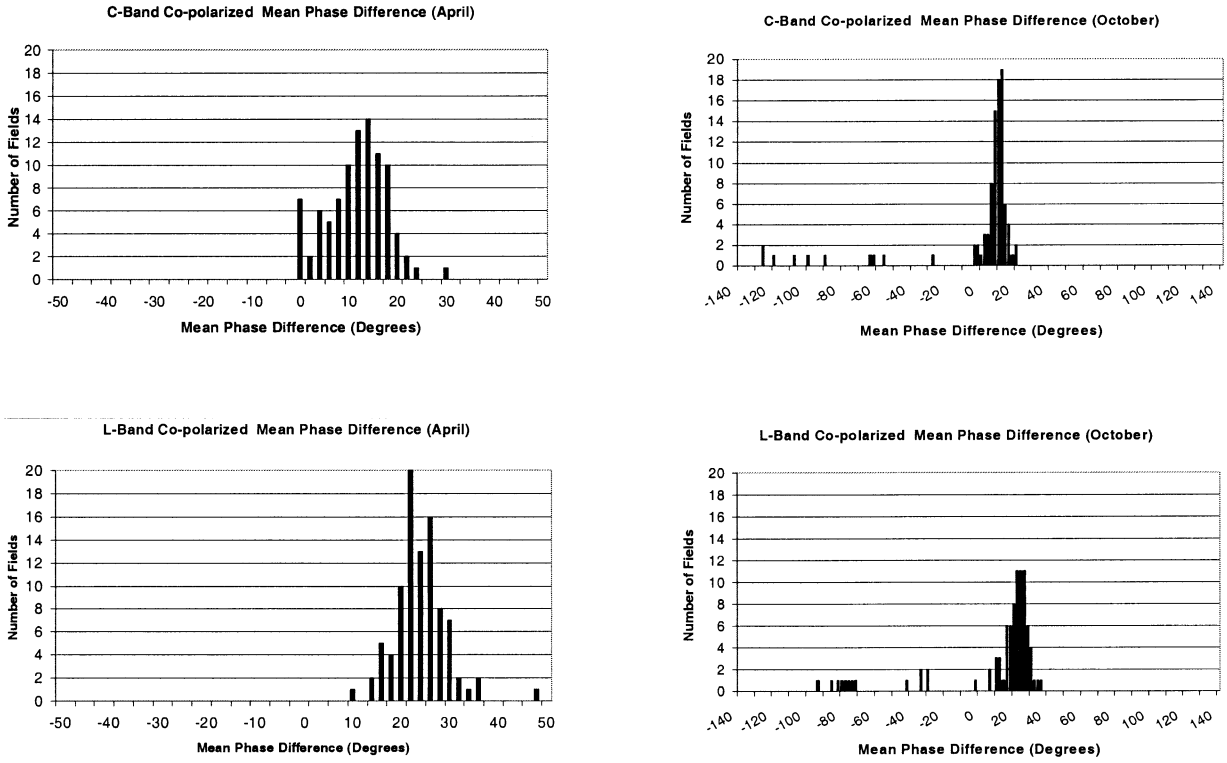

Fig. 2. Frequency distributions for field average PPD. In this figure, the distributions of field average phase differences are plotted for both C- and L-Band results from April and October. In general, phase differences were very similar among all residue fields. In October, fields with standing senesced crops did exhibit phase differences $>30°$.

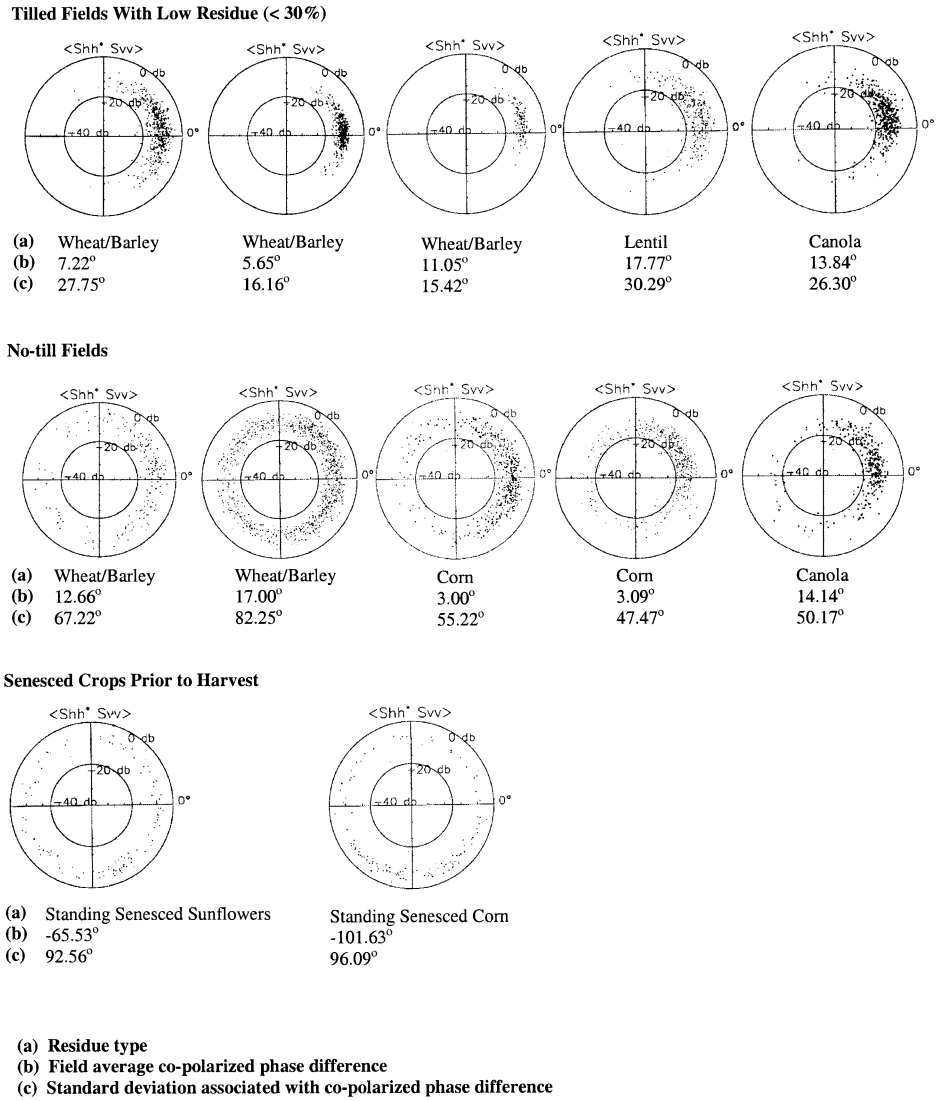

Fig. 3. C-Band PPD distribution plots. These plots demonstrate the distribution of phase differences for individual fields. The accompanying labels provide the field average co-polarized phase distribution, as well as the standard deviation of the phase difference distribution. In general, standing senesced vegetation and no-till fields exhibit broader distributions. Smoother surfaces have small phase differences and narrow distributions.

For the April acquisition where all fields are bare, field average PPD were very similar among all the targets (Fig. 2). The HH/VV phase imbalance for SIR-C is reported to be $\pm 5-10^\circ$ (Freeman et al., 1995). Given this calibration uncertainty, these results suggest that for the fields within the Altona site, the H- and V-polarized waves are more or less in phase. Consequently, mean phase differences provide very little information about soil and residue characteristics. The conditions required to produce a significant phase shift are not present. In October, most fields were harvested and these fields again had very similar phase differences. In contrast, standing senesced corn and sunflower fields had much higher phase differences, although these differences varied significantly between about -30° and -130° at C-Band and between -30° and -90° at L-Band. Ulaby et al. (1987) reported similar phase differences on standing senesced cornfields.

The PPD associated with a pure dihedral reflector will approximate 180°. For distributed targets where more than one scattering source is often present, but significant double-bounce scattering occurs, PPD will approach 180°. The deviation from a PPD of 180° is an indication of the purity of the double-bounce contribution. Kuga and Zhao (1996) suggested that where double-bounce scattering mechanisms are set up, mean phase shifts close to 110° are observed from distributed targets. The PPD observed on the standing senesced corn and sunflower fields within the SIR-C data set suggests that some double-bounce scattering is occurring.

Field average phase differences can distinguish standing senesced crops from harvested fields, but do not distinguish among these residue and tilled fields. However, the field-based phase distribution did provide additional information (Figs. 3 and 4). This distribution varied as a function of the

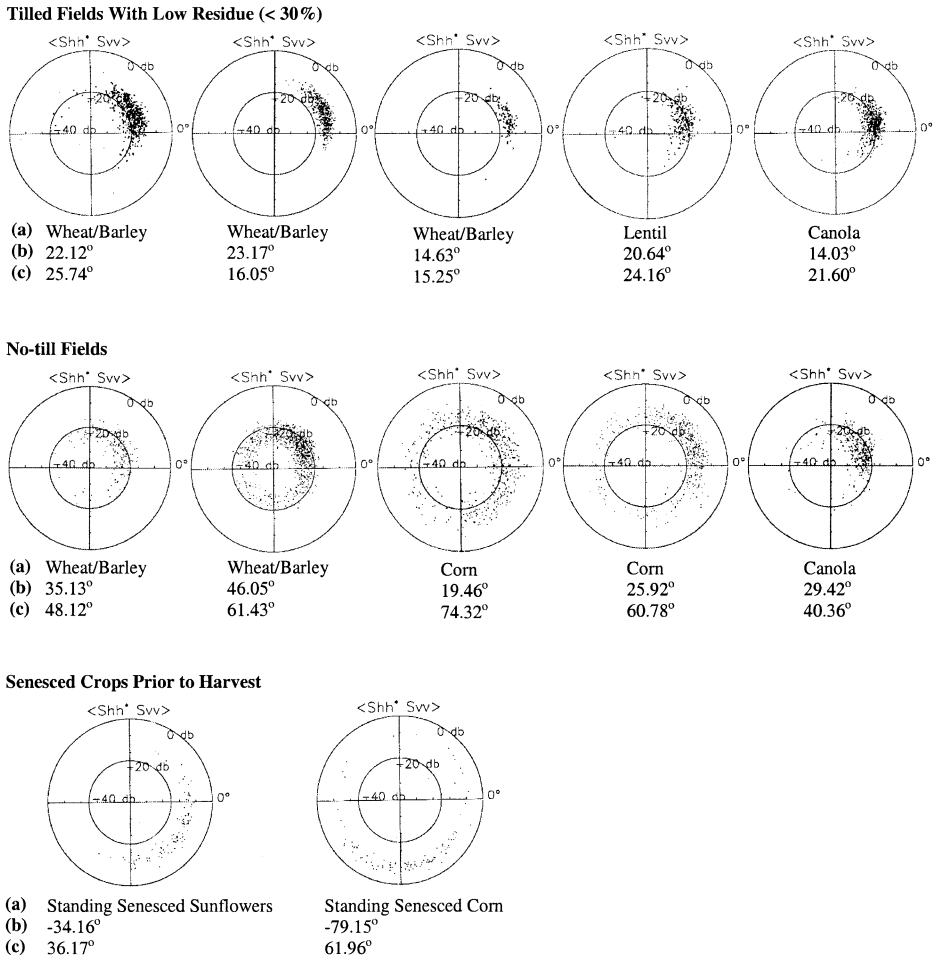

Fig. 4. L-Band PPD distribution plots. These plots demonstrate the distribution of phase differences for individual fields. The accompanying labels provide the field average co-polarized phase distribution, as well as the standard deviation of the phase difference distribution. In general, standing senesced vegetation and no-till fields exhibit broader distributions. Smoother surfaces have small phase differences and narrow distributions.

residue conditions. At C-Band, the PPD distributions, as well as the associated standard deviations, were unique for fields with low residue amounts and for no-till fields. In general, the standard deviation of the phase differences for fields with low residue cover was $< 30°$. This tight distribution is characteristic of surface scattering. In contrast no-till fields had standard deviations $>45°$. For standing senesced crops, field average PPD was higher, and standard deviations were close to $100°$. These crop canopies had phase distribution responses typical of the multiple interactions reported by Evans et al. (1988). Consequently, the PPD distribution suggests that although some double-bounce scattering is occurring, these standing senesced canopies are also experiencing substantial volume scattering.

In comparing standing senesced crops to no-till fields, the mean phase difference approaches $0°$ and the standard deviation is reduced once the crops are harvested. This suggests that the contribution of multiple and volume scattering is reduced once the crop is harvested, and any double-bounce scattering disappears. Nevertheless, the PPD distribution plots indicate that multiple scattering is still present on no-till fields.

Relative to C-Band, mean phase differences for L-Band were slightly higher for all fields with the exception of the standing senesced crops. In contrast to the C-Band results, the distribution of the L-Band PPD was very similar between the standing crops and the no-till fields. These fields generally had broad PPD distributions with significant standard deviations. Tilled fields had narrow distributions similar to the C-Band results. For most fields, the standard deviations were lower at L-Band when compared to C-Band distributions. Sarabandi et al. (1991) also found that the standard deviation associated with the PPD broadens as frequency increases. SIR-C results from the standing cornfields were

similar to results presented in van Zyl (1989), where at large incidence angles L-Band mean phase angles of almost 110° and standard deviations of 63° were observed. L-Band phase differences were slightly less for the data set presented here since the corn canopy was senesced and with penetration deeper into the canopy, more volume and surface scattering is present.

6.3. Interpretation of the co-polarization signature plots

According to the PPD and the distribution of the PPD, harvested fields produce surface and multiple scattering. Standing senesced canopies have a mixture of double-bounce, multiple, and volume scattering. de Matthaeis et al. (1994) describe the co-polarization plots as containing the imprinting by the various scattering mechanisms (surface, double-bounce, and multiple/volume), which combine to yield the global co-polar backscattering for the various polarization states (linear, circular, and elliptical). Thus, these plots encapsulate the scattering characteristics of the target.

Co-polarization signature plots were generated from the SIR-C data for each field surveyed in April and October. To facilitate comparison among these fields, the plots were normalized to the intensity range of 0–1. A sample of typical plots for each of the major cover types is displayed in Figs. 5 and 6. The mean normalized pedestal height was also calculated for the major cover classes and these results are given in Table 4.

A summary of the scattering mechanisms for the main cover types is provided in Table 4. Sources of scattering were determined by examining the shape of the co-polarization plots (polarizations with maximum and minimum responses), the normalized pedestal height, the linear cross-polarized backscatter (HV), and the PPD statistics. Both the linear polarized and circular polarized backscatter also help in the interpretation of the scattering mechanisms present within the target.

6.3.1. Classes of scatterers present at C-Band

6.3.1.1. Fields with little or no residue cover: dominated by surface scattering. According to Dobson and Ulaby (1998), VV and HH responses from smooth surfaces are very similar at angles close to normal incidence, but at larger angles these responses diverge with VV backscatter becoming slightly higher than HH backscatter. On rough surfaces HH and VV backscatter is approximately equal for all incidence angles. In Fig. 5a–e, tilled fields were

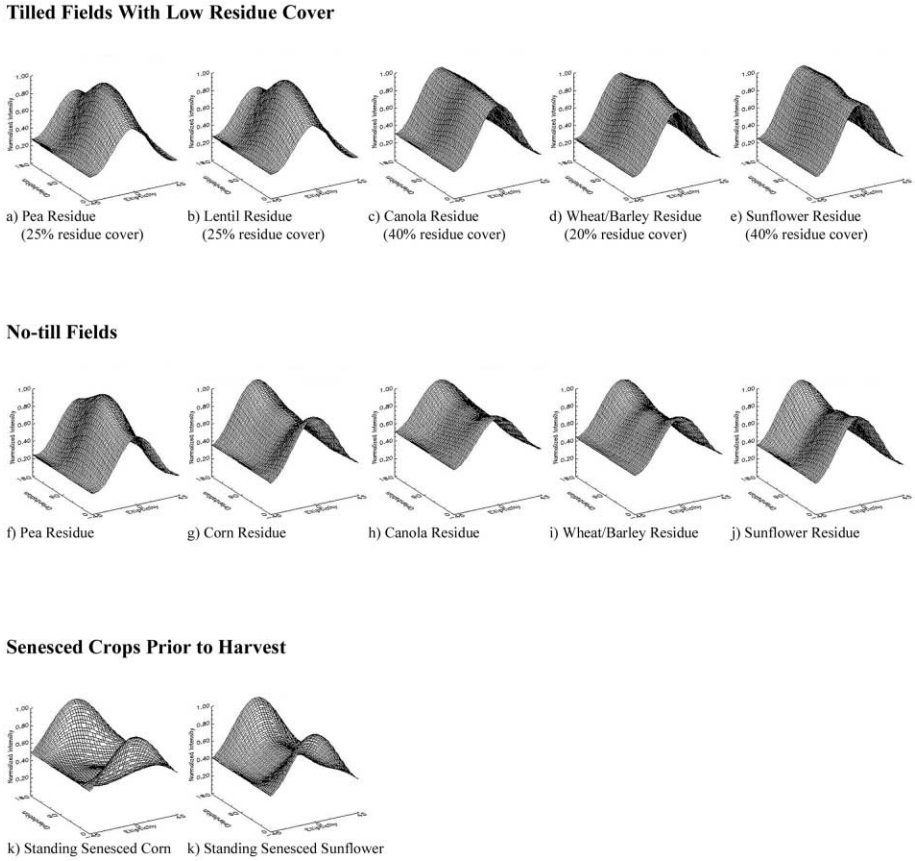

Fig. 5. C-Band co-polarization signature plots. Sample plots presented in this figure are for tilled fields with lower amounts of residue (top) as well as for no-till fields (centre). The figures at the bottom show responses from standing senesced corn and sunflower crops. All plots have been normalized to intensity values between 0 and 1.

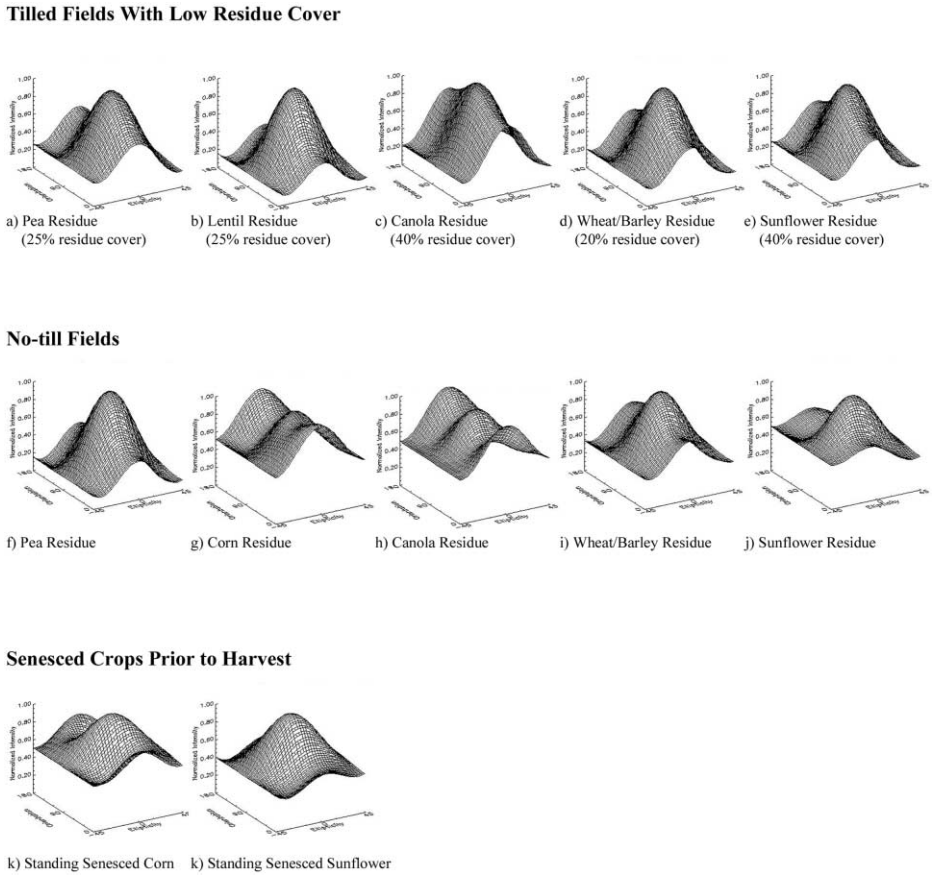

Fig. 6. L-Band co-polarization signature plots. Sample plots presented in this figure are for tilled fields with lower amounts of residue (top) as well as for no-till fields (centre). The figures at the bottom show responses from standing senesced corn and sunflower crops. All plots have been normalized to intensity values between 0 and 1.

split into two classes—those with approximately equal responses at HH and VV and those with slight peaks at VV. These differences suggest that surface roughness varied among these fields. The smoothest fields, those with the finest residue (Fig. 5a and b), have a maximum response at VV. Backscatter was approximately equal at all linear polarizations for the canola, wheat/barley, and sunflower residue fields, suggesting that these fields appear rougher. However, the mean pedestal height (0.29) indicates that fields in this residue class do not

Table 4
General characteristics of the C- and L-Band copolarization signature plots

	Scattering mechanism	HH response relative to VV	Mean normalized pedestal height	
			April	October
C-Band				
Standing senesced crops (corn and sunflower)	double-bounce, volume, and multiple scattering	HH >> VV	–	0.44
No-till (corn, wheat, canola, and sunflower residue)	multiple scattering	HH > VV	0.38	0.38
Tilled (< 50% wheat, canola, and sunflower residue)	surface scattering	HH ≈ VV	0.29	0.32
Tilled (peas and lentil residue)	surface scattering	HH < VV	0.26	–
L-Band				
Standing senesced crops (corn and sunflower)	multiple and volume scattering	HH < VV	–	0.54
No-till (all residue types)	multiple scattering (larger residue) or surface scattering (very fine residue)	HH ≈ VV or HH < VV	0.31	0.35
Tilled (< 50% residue)	surface scattering	HH << VV	0.18	0.24

produce significant depolarization. Thus, the contribution of multiple scattering is limited.

Baronti et al. (1995) predicted that for targets dominated by surface scattering, RL returns will be significantly greater than RR responses. For these tilled fields, RL backscatter was more than 5 dB higher than RR backscatter, confirming the presence of significant surface scattering. As presented in Fig. 3, the average PPD was close to 0° for this class of fields and PPD distributions were narrow. These PPD statistics and the low pedestal height indicate that relative to the other fields, only a very small part of the incident wave becomes unpolarized during scattering. Thus, although some multiple scattering is likely still occurring as a result of surface roughness and a small amount of residue, surface scattering is the most important mechanism on these fields.

6.3.1.2. No-till residue fields: dominated by multiple scattering. HH backscatter was slightly higher than VV backscatter for most of the no-till fields. As a result, the co-polarization plots for these fields have a noticeable saddle shape (Fig. 5g–j). Although these plots are characteristic of double-bounce scatterers (van Zyl et al., 1987), multiple interactions are likely the dominant scattering source. The pedestal height on these co-polarization plots was larger (0.38) and thus, more depolarization is occurring on the no-till fields relative to the tilled fields with low residue cover. Also indicative of multiple scattering, RL backscatter was higher than RR backscatter. According to Baronti et al. (1995), when surface scattering dominates RL>>RR, but this difference is reduced in the presence of significant multiple scattering (RL>RR). On these no-till fields, the circular cross-polarized (RL) backscatter was greater than the co-polarized (RR) backscatter, but this difference was approximately 2 dB. This compares to the >5-dB difference observed on fields with surface scattering.

The importance of multiple scattering on these no-till fields is not obvious from the field average PPD. The mean PPD for these targets is close to 0°, and thus as concluded from the regression analysis, average PPD is not sensitive to roughness and residue conditions. The random PPD distributions do, however, support the conclusion that multiple scattering is occurring (Fig. 3).

The polarization signature plot for the no-till pea residue field (Fig. 5f) was different than the other no-till surfaces. Peas leave less residue after harvest and this residue also tend to be very fine. Although this field had not been tilled, the recorded response was very similar to the pea residue field that had been tilled (Fig. 5a). These observations suggest that very fine residue has little effect on radar response and that this target appears smooth at C-Band.

6.3.1.3. Unharvested senesced crops: a combination of double-bounce, multiple, and volume scattering. Standing senesced corn and sunflower fields, like the no-till corn, canola, wheat/barley, and sunflower fields produced saddle shaped co-polarization plots (Fig. 5k–l). Groot, van den Broek, and Freeman (1992) observed similar responses for crops such as wheat that had narrow, elongated stems. de Matthaeis et al. (1991) found similar saddle shaped features for corn crops. The difference between the HH and VV responses for the standing senesced crops was larger when compared to the postharvest corn and sunflower targets. The saddle on the plots generated for these standing crops is deeper and double-bounce reflections are likely occurring within the crop canopies. The mean PPD for the standing senesced cornfields approached 100° (Fig. 3), and RL backscatter was approximately equal to RR backscatter. These observations support the presence of double-bounce scattering (Baronti et al., 1995).

Other SAR parameters suggest that multiple or volume scattering sources are also present in these canopies. As with the no-till fields, the pedestal height is significant for the standing senesced crops. The pedestal indicates that as a result of volume and multiple scattering, the polarization changes randomly within these targets. The pedestal height was greatest for the standing senesced crops (0.44), decreased on the no-till fields (0.38), and was lowest for the tilled fields (0.29). Unharvested crops have a greater volume of vegetative material relative to the no-till residue targets. The pedestal height indicates that for standing senesced crops, at least 40% of the response is unpolarized. In addition, the distribution of the PPD was typical of targets that result in multiple and volume scattering.

6.3.2. Classes of scatterers present at L-Band

6.3.2.1. Tilled fields with low residue cover: dominated by surface scattering. Fields that had been tilled or had very fine residue cover exhibited responses typical of surface scattering targets (Fig. 6a–e). For these targets, maximum response is at an orientation of 90° and the target appears flat relative to the wavelength. For these fields, the low pedestal heights (0.18–0.24) indicate minimal depolarization and thus confirm that surface scattering is dominant. These surfaces are not rough enough and do not have enough vegetative material to cause significant multiple or volume scattering. The difference between VV and HH backscatter is much more pronounced at L-Band relative to C-Band since these surfaces appear much smoother at this longer wavelength.

The circular polarization responses and the PPD results also support the conclusion that these surfaces are experiencing surface scattering. Typical of surface scatterers, RL responses were more than 4 dB higher than responses recorded for RR. The mean PPD and the standard deviation of the PPD were small. Both statistics support the conclusion that surface scattering occurs on these fields.

6.3.2.2. No-till residue fields and unharvested senesced crops: dominated by multiple and volume scattering. The L-Band co-polarization plots for no-till fields (Fig. 6f–j) and for fields of standing senesced crops (Fig. 6k–l) were

very different when compared to C-Band responses. The relationship between the maximum and minimum linear polarization responses (VV>HH) is indicative of targets considered smooth relative to the longer L-Band wavelength. If only the linear co-polarization configurations were examined, these fields could be confused with fields with low residue cover. However, the pedestal height and the distribution of the PPD differentiate these no-till and standing cropped targets. The pedestal height was largest for standing senesced and no-till corn and sunflower fields. Although the linear polarizations suggest surface scattering, the pedestal height indicates that polarization does vary randomly within these targets, and that multiple and volume scattering is still an important component even at L-Band. From the PPD distributions it appears that the contribution of multiple and volume scattering likely varies among these fields, since the standard deviations range from $<40°$ to $>70°$ (Fig. 4). However, mean phase differences for the standing senesced fields was much lower relative to C-Band and therefore, double-bounce scattering has been substantially reduced. As with the C-Band results, no-till pea residue plots were more characteristic of tilled fields with low residue cover.

7. Conclusions

This article reported on results from the analysis of polarimetric SIR-C data. The data were acquired over an agricultural test site during the period of preplanting and postharvest. Simple regression results demonstrated that residue cover, and in particular surface roughness, affect polarimetric responses. C- and L-Band radar parameters sensitive to volume and multiple scattering were most sensitive to these target characteristics. These radar parameters included pedestal height, as well as the linear cross-polarization (HV) and the circular co-polarization (RR). The multivariate model that related pedestal height to soil and residue properties produced the best results. The coefficient of determination for C- and L-Band pedestal height approached or exceeded 0.9.

The importance of pedestal height was also evident in the C- and L-Band co-polarization signature plots. Several types of scattering are usually present within distributed targets, although these targets often have a dominant scattering mechanism. Both the shape of the co-polarization signature plots and the pedestal on which the plots sit provide information on the dominant scattering mechanism. The polarization signature plots clearly differentiated these agricultural fields based on the type of scattering. The scattering mechanisms associated with standing senesced vegetation, no-till fields, and tilled fields varied. Double-bounce, multiple, and volume scattering were all present in standing vegetation, while for no-till fields multiple scattering dominated. Surface scattering was most important on fields that had been tilled, or had very fine and sparse residue cover. The pedestal height was also unique for each of these classes, with larger pedestals associated with standing crops and no-till fields. This confirms the sensitivity of pedestal height to multiple and volume scattering.

Mean PPD were close to $0°$ for most residue fields and thus this statistic provided little useful information for this application. Standing senesced crops did exhibit phase differences significantly greater than $0°$ although mean phase differences varied among these fields. The phase differences confirm that some double-bounce scattering occurs on cropped fields, even when the crop is senesced. More information is provided by the PPD distributions and the standard deviation associated with these distributions. Broad phase distributions were typical of no-till fields and standing senesced vegetation.

Although satellite SAR sensors capable of acquiring fully polarimetric data are not currently available, the launch of systems with this type of complex capability is planned. These planned sensors include both the Canadian RADARSAT-2 (C-Band) and the Japanese PALSAR (L-Band). Published research into the application of polarimetric data for mapping distributed targets is limited. Thus, results presented in this article, from the analysis of SIR-C data, provide a significant contribution to this body of knowledge.

Acknowledgments

Dr. Joost van der Sanden from the Canada Centre for Remote Sensing provided a valuable review of this manuscript.

References

Baronti, S., Del Frate, F., Ferrazzoli, P., Paloscia, S., Pampaloni, P., & Schiavon, G. (1995). SAR polarimetric features of agricultural areas. *International Journal of Remote Sensing*, *14*, 2639–2656.

Boerner, W. M., Foo, B. Y., & Eom, H. J. (1987). Interpretation of the polarimetric co-polarization phase term in radar images obtained with the JPL airborne L-Band SAR system. *IEEE Transactions on Geoscience and Remote Sensing*, *25*, 77–81.

Boerner, W. M., Mott, H., Lüneburg, E., Livingstone, C., Brisco, B., Brown, R. J., & Paterson, J. S. (1998). Polarimetry in radar remote sensing: basic and applied concepts. In: F. M. Henderson, & A. J. Lewis (Eds.), *Principles and applications of imaging radar, manual of remote sensing, vol. 2* (3rd ed., pp. 271–357). New York: Wiley.

Brisco, B., Brown, R. J., Snider, B., Sofko, G. J., Koehler, J. A., & Wacker, A. G. (1991). Tillage effects on the radar backscattering coefficient of grain stubble fields. *International Journal of Remote Sensing*, *12*, 2283–2298.

Coleman, D., & Roberts, R. (1987). *Report on cropping, tillage and land management practices in Southwestern Ontario: 1986, Soil and Water Environmental Enhancement Program (SWEEP)* (82 pp.).

de Matthaeis, P., Ferrazzoli, P., Guerriero, L., Schiavon, G., Solimini, D., & Tognolatti, P. (1991). Radar response to vegetation parameters: comparison between theory and MAESTRO-1 results. In: *Proceedings of the International Geoscience and Remote Sensing Symposium (IGARSS '91), Geoscience & Remote Sensing Society, Espoo, Finland* (pp. 685–688).

de Matthaeis, P., Ferrazzoli, P., Schiavon, G., & Solimini, D. (1992). Agriscatt and MAESTRO: multifrequency radar experiments for vegetation remote sensing. In: *Proceedings of MAESTRO-1/AGRISCATT: Radar Techniques for Forestry and Agricultural Applications, Final Workshop, The Netherlands* (pp. 231–248). Paris, France: European Space Agency.

de Matthaeis, P., Schiavon, G., & Solimini, D. (1994). Effect of scattering mechanisms on polarimetric features of crops and trees. *International Journal of Remote Sensing*, *15*, 2917–2930.

Dobson, M. C., & Ulaby, F. T. (1998). Mapping soil moisture distribution with imaging radar. In: F. M. Henderson, & A. J. Lewis (Eds.), *Principles and applications of imaging radar, manual of remote sensing, vol. 2* (3rd ed., pp. 407–433). New York: Wiley.

Evans, D. L., Farr, T. G., van Zyl, J. J., & Zebker, H. A. (1988). Radar polarimetry: analysis tools and applications. *IEEE Transactions on Geoscience and Remote Sensing*, *26*, 774–789.

Freeman, A., Alves, M., Chapman, B., Cruz, J., Kim, Y., Shaffer, S., Sun, J., Turner, E., & Sarabandi, K. (1995). SIR-C data quality and calibration results. *IEEE Transactions on Geoscience and Remote Sensing*, *33*, 848–857.

Groot, J. S., van den Broek, A. C., & Freeman, A. (1992). An investigation of the potential of polarimetric SAR data for discrimination between agricultural crops. In: *Proceedings of MAESTRO-1/AGRISCATT: Radar Techniques for Forestry and Agricultural Applications, Final Workshop, The Netherlands* (pp. 67–82). Paris, France: European Space Agency.

Hoekman, D. H., van der Sanden, J. J., & Vissers, M. A. M. (1992). MAESTRO-1 Flevoland/Speulderbos: analysis results of multiband polarimetric SAR data of forests and agricultural crops. In: *Proceedings of MAESTRO-1/AGRISCATT: Radar Techniques for Forestry and Agricultural Applications, Final Workshop, The Netherlands* (pp. 53–58). Paris, France: European Space Agency.

Johnson, F., Brisco, B., & Brown, R. J. (1993). Evaluation of limits to the performance of the surface roughness meter. *Canadian Journal of Remote Sensing*, *19*, 140–145.

Kuga, Y., & Zhao, H. (1996). Experimental studies on the phase distribution of two co-polarized signal scattered from two-dimensional rough surfaces. *IEEE Transactions on Geoscience and Remote Sensing*, *34*, 601–603.

McNairn, H., Boisvert, J. B., Major, D. J., Gwyn, Q. H. J., Brown, R. J., & Smith, A. M. (1996). Identification of agricultural tillage practices from C-Band radar backscatter. *Canadian Journal of Remote Sensing*, *22*, 154–162.

McNairn, H., Ellis, J., van der Sanden, J. J., Hirose, T., & Brown, R. J. (2001). Providing crop information using RADARSAT-1 and satellite optical imagery. *International Journal of Remote Sensing (*in press).

McNairn, H., van der Sanden, J. J., Brown, R. J., & Ellis, J. (2000). The potential of RADARSAT-2 for crop mapping and assessing crop condition. In: *Proceedings of the Second International Conference on Geospatial Information in Agriculture and Forestry, Lake Buena Vista, FL*, (vol. II, pp. pp. 81–88)). Ann Arboue, USA: ERIM International Inc.

Pultz, T., Crevier, Y., Brown, R. J., & Boisvert, J. (1997). Monitoring local environmental conditions with SIR-C/X-SAR. *Remote Sensing of Environment*, *59*, 248–255.

Ray, T. W., Farr, T. G., & van Zyl, J. J. (1992). Polarization signatures for abandoned agricultural fields in the Manix Basin area of the Mojave Desert: can polarimetric SAR detect desertification? In: *Proceedings of the International Geoscience and Remote Sensing Symposium (IGARSS '92), Geoscience & Remote Sensing Society, Houston* (pp. 947–949).

Richards, B. K., Walter, M. F., & Muck, R. E. (1984). Variation in the line transect measurements of crop residue cover. *Journal of Soil and Water Conservation*, *39*, 66–67.

Sarabandi, K., Oh, Y., & Ulaby, F. T. (1991). Polarimetric radar measurements of bare soil surfaces at microwave frequencies. In: *Proceedings of the International Geoscience and Remote Sensing Symposium (IGARSS '91), Geoscience & Remote Sensing Society, Espoo, Finland* (pp. 387–390).

Stofan, E. R., Evans, D. L., Schmullius, C., Holt, B., Plaut, J. J., van Zyl, J., Wall, S. D., & Way, J. (1995). Overview of results of Spaceborne Imaging Radar-C, X-Band Synthetic Aperture Radar (SIR-C/X-SAR). *IEEE Transactions on Geoscience and Remote Sensing*, *33*, 817–828.

Topp, G. C., Davis, J. L., & Annan, A. P. (1980). Electromagnetic determination of soil water content: measurements in coaxial transmission lines. *Water Resources Research*, *16*, 547–582.

Ulaby, F. T., Held, D., Dobson, M. C., McDonald, K. C., & Senior, T. B. A. (1987). Relating polarization phase difference of SAR signals to scene properties. *IEEE Transactions on Geoscience and Remote Sensing*, *25*, 83–92.

van der Sanden, J. J., Budkewitsch, P., Landry, R., Manore, M. J., McNairn, H., Pultz, T. J., & Vachon, P. W. (2000). Application potential of planned SAR satellites—a preview. In: *Proceedings of the 22nd Canadian Remote Sensing Symposium, Victoria, Canada* [CD-ROM]. Ottawa, Canada: Canadian Aeronautics & Space Institute.

van Zyl, J. J. (1989). Unsupervised classification of scattering behaviour using radar polarimetry data. *IEEE Transactions on Geoscience and Remote Sensing*, *27*, 36–45.

van Zyl, J. J., Zebker, H. A., & Elachi, C. (1987). Imaging radar polarization signatures: theory and observation. *Radio Science*, *22*, 529–543.